INTERNATIONAL JOURNAL FOR NUMERICAL METHODS IN FLUIDS, VOL. 9, 855–864 (1989)

A TOTAL PRESSURE CORRECTION FOR UPSTREAM WEIGHTED SCHEMES

V. DE HENAU, G. D. RAITHBY AND B. E. THOMPSON*

Department of Mechanical Engineering, University of Waterloo, Waterloo, Ontario, Canada, N2L 3G1

SUMMARY

Upwind differencing is known to lead to a substantial loss in total pressure. The present paper illustrates the importance of this error on two problems: flow in a converging–diverging duct and flow around a cylinder. A correction is proposed that reduces the total pressure error and yields dramatically improved results for the test problems.

KEY WORDS Finite volume method Accurate total pressure prediction Discretization accuracy

1. INTRODUCTION

Discrete methods for solving fluid flow problems often estimate the value of the variables at control volume faces in terms of the nodal values using some upstream weighted approximation. This approach provides stable schemes but can also lead to serious errors such as false diffusion[1] and loss of total pressure.[2] Another type of error, related to grid curvature,[3] is also associated with the upstream approximation. Lillington[4] recognized that a streamwise correction to any upstream approximation scheme is required to enhance accuracy. Galpin *et al.*[5] clearly demonstrated the connection between such a correction and the total pressure error.

In the present paper, a correction to the upstream weighted average scheme of Raithby and Torrance[6] is discussed. The objective of the correction is to reduce the total pressure error that results from the application of the upstream scheme to the discretization of the momentum equations. This paper demonstrates the importance of eliminating the total pressure error. The particular method that is used applies well to situations where the main flow direction is closely aligned with the grid lines.

2. THE TOTAL PRESSURE CORRECTION

The source of the total pressure error and a remedy to it for one-dimensional inviscid flows are discussed by Galpin *et al.*[5] The present approach differs in that the correction is based on the local solution of the one-dimensional viscous flow problem illustrated in Figure 1. The momentum equation for that problem can be written as

$$\frac{\rho U}{\mu}\frac{\mathrm{d}U}{\mathrm{d}x} - \frac{\mathrm{d}^2U}{\mathrm{d}x^2} = -S, \tag{1}$$

* Present address: Scientific Research Associates, Glastonbury, CT, U.S.A.

0271–2091/89/070855–10$05.00

Received 30 June 1988
Revised 2 November 1988

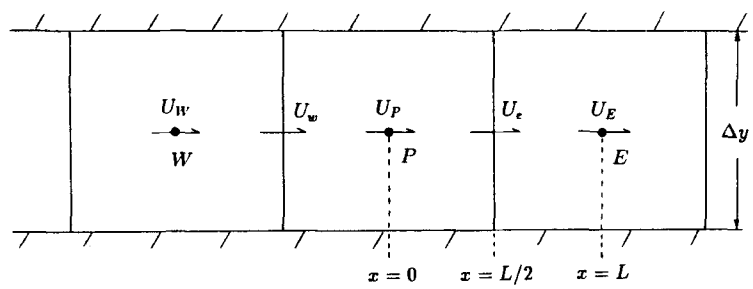

Figure 1. One-dimensional flow problem used to derive the total pressure correction

where ρU is taken as constant over $0 \leqslant x \leqslant L$. The boundary conditions are

$$\text{at } x = 0, \qquad U = U_P,$$

$$\text{at } x = L, \qquad U = U_E.$$

The source S contains the influence of the pressure gradient and of the shear. S is assumed constant over the interval $0 \leqslant x \leqslant L$ and is given by

$$S = \frac{1}{\mu}\frac{\partial P}{\partial x} - \frac{\partial^2 U}{\partial y^2}. \tag{2}$$

The solution to equation (1) with the given boundary conditions yields[7]

$$U = U_P\left[\frac{e^{Re(x/L)} - e^{Re}}{1 - e^{Re}}\right] + U_E\left[\frac{1 - e^{Re(x/L)}}{1 - e^{Re}}\right] - \frac{SL}{Re}\left[x - L\left(\frac{1 - e^{Re(x/L)}}{1 - e^{Re}}\right)\right], \tag{3}$$

where

$$Re = \dot{M}L/\mu\Delta y, \qquad \dot{M} = \rho U \Delta y.$$

Hence, at the east face of the P velocity control volume (at $x = L/2$ in Figure 1) for example, the velocity is

$$U_e = \underbrace{(\tfrac{1}{2} + \alpha_e)U_P + (\tfrac{1}{2} - \alpha_e)U_E}_{\text{I}} - \underbrace{S\alpha_e L^2/Re}_{\text{II}}, \tag{4}$$

where

$$\alpha_e = \frac{1}{2} - \left(\frac{1 - e^{Re/2}}{1 - e^{Re}}\right). \tag{5}$$

The Reynolds number in equations (4) and (5) is based on the mass flow through the east face of the control volume. A similar expression is obtained for the west face velocity.

The weighted average scheme of Raithby and Torrance[6] expresses the face velocity using only term I of equation (4), which is also equivalent to the scheme proposed by Spalding.[8] In other words, the scheme neglects the effects of the pressure gradient and of the shear on the velocity change between the node P and the face. The omission of term II results in the total pressure error.

It is interesting to note that for the particular case of an inviscid flow (i.e. $\mu \to 0$), $\alpha_e = \frac{1}{2}$ and, from equation (2),

$$\lim_{\mu \to 0} \frac{S\alpha_e L^2}{Re} = \frac{L\Delta y}{2\dot{M}_e}\frac{\partial P}{\partial x}.$$

Equation (4) can then be written as

$$U_e = U_P - \frac{L\Delta y}{2\dot{M}_e}\frac{\partial P}{\partial x}. \tag{6}$$

Equation (6) is identical to the correction proposed by Galpin *et al.*[5] for the special case of one-dimensional inviscid duct flow.

The total pressure correction presented in this section is based on the solution of a one-dimensional problem. The correction will be accurate if the flow is closely aligned with one of the grid line directions ($V \approx 0$) or if the cross-stream gradient in V (i.e. $\partial U/\partial y$) is small. If $V\partial U/\partial y$ is large, failure to add the cross-stream advection term will result in a false diffusion error.

Finally, the influence of the cross-stream diffusion is included in the source S (equation (2)) because of test results which indicated that, for viscous flows, the streamwise pressure gradient and the shear stress were of the same order of magnitude near solid walls.[9]

3. DISCRETIZATION OF THE TOTAL PRESSURE CORRECTION

The two-dimensional momentum equations can be written in general orthogonal co-ordinates and discretized by a finite volume approach.[10] Based on the co-ordinate system illustrated in Figure 2(a), the net momentum flux in the x_1-direction for the velocity control volume surrounding U_P (region enclosed by dashed lines in Figure 2(a)) can be expressed as[11]

$$\int_{x_2}\int_{x_1}\frac{1}{h_1h_2}\frac{\partial}{\partial x_1}(\rho h_2 UU)h_1h_2\,dx_1\,dx_2 \approx \dot{M}_e U_e - \dot{M}_w U_w.$$

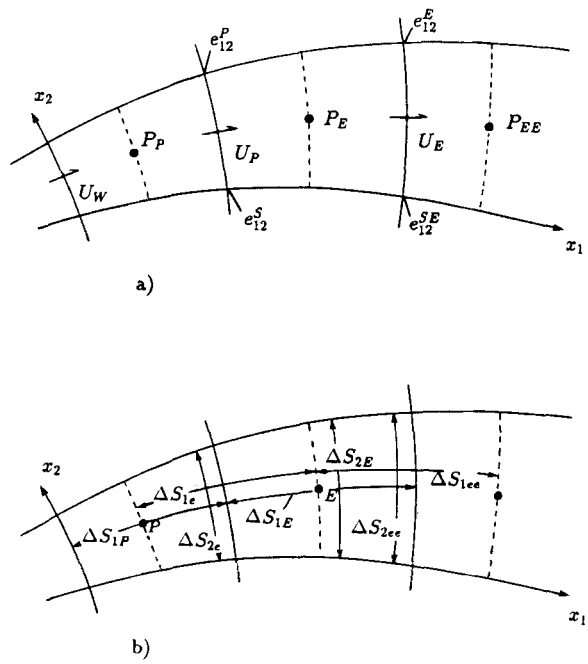

Figure 2. (a) General orthogonal co-ordinate system with storage locations for velocity U, pressure P and shear strains e_{12}; (b) general orthogonal co-ordinate system with storage convention for arc lengths

Substituting equation (4) for the face velocities, the following is obtained:

$$\begin{aligned}\dot{M}_e U_e - \dot{M}_w U_w = {} & \dot{M}_e[(\tfrac{1}{2}+\alpha_e)U_P + (\tfrac{1}{2}-\alpha_e)U_E] \\ & - \dot{M}_w[(\tfrac{1}{2}+\alpha_w)U_W + (\tfrac{1}{2}-\alpha_w)U_P] \\ & \underbrace{- \dot{M}_e\left(\frac{S\alpha}{Re}\right)_e (\Delta S_{1E})^2}_{A} \underbrace{+ \dot{M}_w\left(\frac{S\alpha}{Re}\right)_w (\Delta S_{1P})^2}_{B}. \end{aligned} \tag{7}$$

Terms A and B in equation (7) form the total pressure correction for the net advection of momentum across the control volume in the main flow direction. The east face correction (term A) can be written as

$$\dot{M}_e\left(\frac{S\alpha}{Re}\right)_e (\Delta S_{1E})^2 = \frac{\dot{M}_e \alpha_e (\Delta S_{1E})^2}{(Re)_e}\left(\frac{1}{\mu}\frac{\partial P}{\partial x} - \frac{\partial^2 U}{\partial y^2}\right)_e. \tag{8}$$

Referring to Figures 2(a) and 2(b), the approximations to the different terms of equation (8) are

$$(Re)_e = \frac{\dot{M}_e \Delta S_{1E}}{\mu \Delta S_{2E}},$$

$$\left(\frac{\partial P}{\partial x}\right)_e \approx \frac{P_{EE} - P_P}{\Delta S_{1e} + \Delta S_{1ee}},$$

$$\left(\frac{\partial^2 U}{\partial y^2}\right)_e \approx \frac{1}{2}\left(\frac{e_{12}^P - e_{12}^S}{\Delta S_{2e}} + \frac{e_{12}^E - e_{12}^{SE}}{\Delta S_{2ee}}\right),$$

where e_{12} represents the strain rate. Analogous approximations are used for the west face correction.

4. VERIFICATION OF THE PERFORMANCE OF THE CORRECTION

4.1. The converging–diverging duct problem

A good test problem to evaluate the performance of the total pressure correction is the laminar flow in a converging–diverging duct. For that particular problem, the pressure gradient in the main flow direction forms an important part of the momentum balance. It is therefore expected that the use of an upwind scheme without any correction will lead to a significant total pressure error.

The geometry of the problem as well as the boundary conditions and the fluid properties are illustrated in Figure 3. The equations are discretized following the method of Raithby *et al.*[11] for orthogonal grids. Two different grid sizes, denoted by $N \times 10$, are used. N and 10 are the number of pressure nodes[11] in the x_1-and x_2-direction respectively. N is chosen to be 18 and 36 for the two grids used.

Along the centre line of the duct, the velocity in the x_2-direction is zero. The x_1-momentum equation can therefore be expressed as

$$\rho U \frac{\partial U}{\partial x_1} + \frac{\partial P}{\partial x_1} - \mu \frac{\partial^2 U}{\partial x_1^2} - \mu \frac{\partial^2 U}{\partial x_2^2} = 0, \tag{9}$$

where the grid curvature terms are neglected. Integrating equation (9) along x_1 from, say, point A

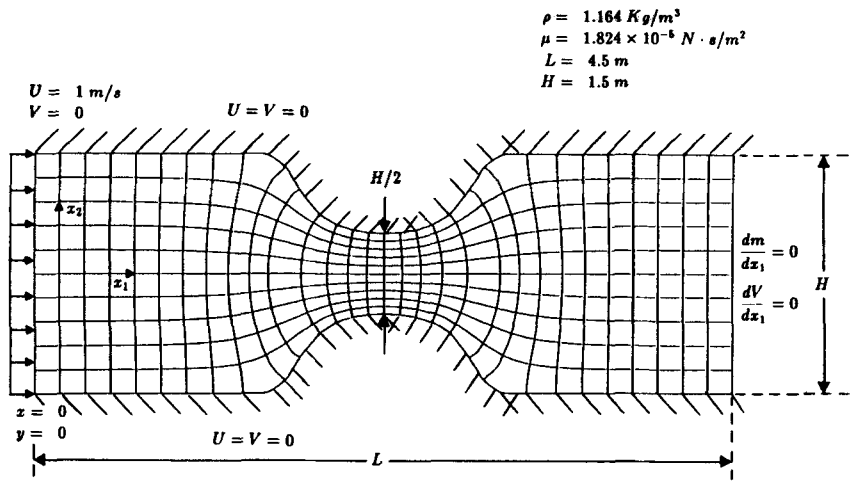

Figure 3. Converging–diverging duct problem: geometry, properties of fluid and boundary conditions

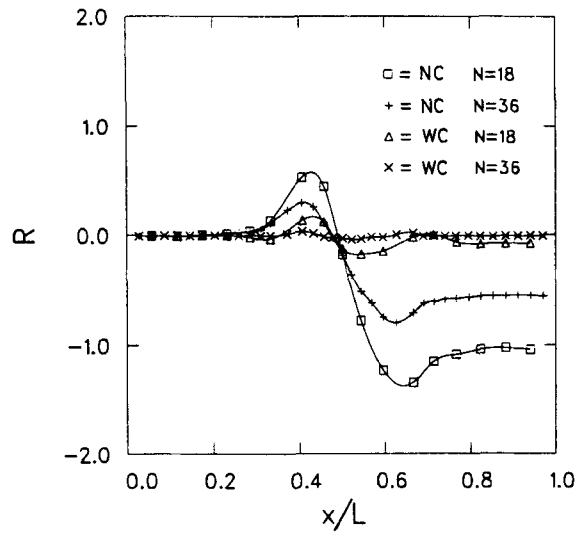

Figure 4. Total pressure variation along centre line of converging–diverging duct using an upwind scheme (NC) and an upwind scheme with the total pressure correction (WC) for different numbers of control volumes in x_1

to point B yields the following expression:

$$\tfrac{1}{2}\rho(U_B^2 - U_A^2) + (P_B - P_A) - \mu \int_A^B \left(\frac{\partial^2 U}{\partial x_1^2} + \frac{\partial^2 U}{\partial x_2^2} \right) dx_1 = R. \tag{10}$$

R represents a 'total pressure' change between points A and B. If equation (9) is satisfied exactly, R is zero.

Figure 4 illustrates the R-profiles obtained using the 'standard' upstream weighted average scheme of Raithby and Torrance[6] with no correction (NC). Also shown are the profiles obtained with the same upstream scheme corrected with the total pressure correction (WC).

A significant error (i.e. departure of R from zero) appears after the contraction when NC is used. By increasing the number of nodes in the x_1-direction (i.e. decreasing ΔS_1), the error decreases. R is proportional to ΔS_1,[5] and it is expected that R will asymptotically vanish as N increases.

The magnitude of R is dramatically reduced when WC is used. For $N = 18$ the difference between the outlet and inlet dynamic heads is reduced from about 170% to 12%. For $N = 36$ the difference is less than 1%.

It is important to mention that false diffusion does not give rise to significant error because the flow is closely aligned with the grid lines.

In the present situation the flow is two-dimensional; but, by taking advantage of the fact that the main flow direction is closely aligned with the grid lines, the application of the correction allows a significant reduction of the total pressure error with a reasonable number of control volumes.

4.2. Potential flow past a cylinder

Because of the presence of large pressure gradients, the potential flow past a cylinder is another excellent test problem for the total pressure correction. The geometry of the problem and the properties of the fluid are given in Figure 5.

The analytical streamwise velocity for the potential flow around a cylinder in an infinite domain is given by[12]

$$\frac{U_s}{U_\infty} = \left(1 + \frac{a^2}{r^2} - 2\frac{a^2}{r^2}\cos(2\theta)\right)^{1/2}. \tag{11}$$

Here r and θ are the polar co-ordinates of the point where U_s is sought.

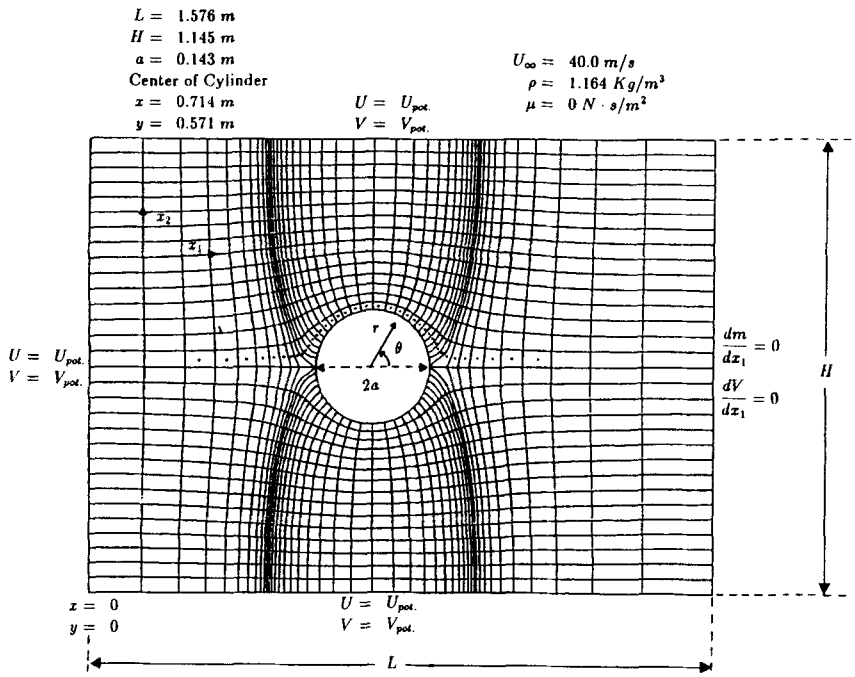

Figure 5. Potential flow past a cylinder problem: geometry, properties of fluid and boundary conditions

The pressure coefficient C_p is defined as

$$C_p = \frac{P - P_\infty}{\frac{1}{2}\rho_\infty U_\infty^2}.$$

From Bernoulli's equation

$$P_\infty + \tfrac{1}{2}\rho_\infty U_\infty^2 = P + \tfrac{1}{2}\rho U_s^2,$$

the pressure coefficient can be rewritten in incompressible form as

$$C_p = 1 - U_s^2/U_\infty^2, \tag{12}$$

with U_s/U_∞ given by equation (11).

The numerical calculation is performed on a 40 × 30 orthogonal grid. The boundary velocities are specified from the analytical solution, except at the outflow boundary where a fully developed flow is assumed. As with the previous test problem, the transport equations for momentum are discretized by the method of Raithby *et al.*[11] In the estimation of mass flows across all control volumes faces, however, a linear variation of velocity with distance along the faces was used. This approach yields more accurate estimates of the mass flow rates, particularly for the regions near the stagnation points. Full details of the discretization of the equations are available in the thesis of De Henau.[9]

Figures 6(a) and 6(b) compare the calculated and analytical results (equations (11) and (12)) for the dimensionless streamwise velocity U_s/U_∞ and the pressure coefficient C_p. The comparison is done at the pressure nodes *within* the flow that lie adjacent to the plane of symmetry and to the surface of the cylinder. Some sample pressure nodes are illustrated in Figure 5 by dots within the control volumes. It is noted that, from equation (11), U_s/U_∞ should lie between 0·0 and 2·0 on the surface of the cylinder (for $r = a$). However, because the points where the comparison is made do not lie on the surface of the cylinder, the maximum value of U_s/U_∞ is less than 2·0 and the minimum greater than 0·0, as illustrated in Figure 6(a). The same applies for the maximum value of C_p which is less than 1·0 and the minimum which is greater than $-3{\cdot}0$ (Figure 6(b)). The curves labelled WC and NC refer respectively to the calculations performed with and without the pressure correction.

The numerical results obtained applying the total pressure correction are in excellent agreement with the analytical results. The small discrepancies observed near the stagnation points and at the top (or bottom) of the cylinder are attributed to the poor grid resolution in those regions of high gradients.

As illustrated in Figure 6(a), a velocity deficit of about 20% is observed behind the cylinder when the pressure correction is not applied. Figure 6(b) indicates that the omission of the correction results in a pressure loss near the trailing edge of the cylinder. Those results once again indicate the importance of the total pressure correction when an upstream scheme is used.

5. DISCUSSION AND CONCLUSIONS

The standard upstream weighted scheme obtains the velocity U_e at the control volume face that lies between the nodes for the velocities U_P and U_E, by solving a one-dimensional advection–diffusion equation. The present paper improves the accuracy of this scheme by including the effects of the pressure gradient and cross-stream diffusion in the one-diemensional solution. This scheme will therefore give more accurate pressures than the standard upstream scheme whether or not the flow is aligned with the grid, but will be subject to a false diffusion error when the flow crosses the grid at an angle.

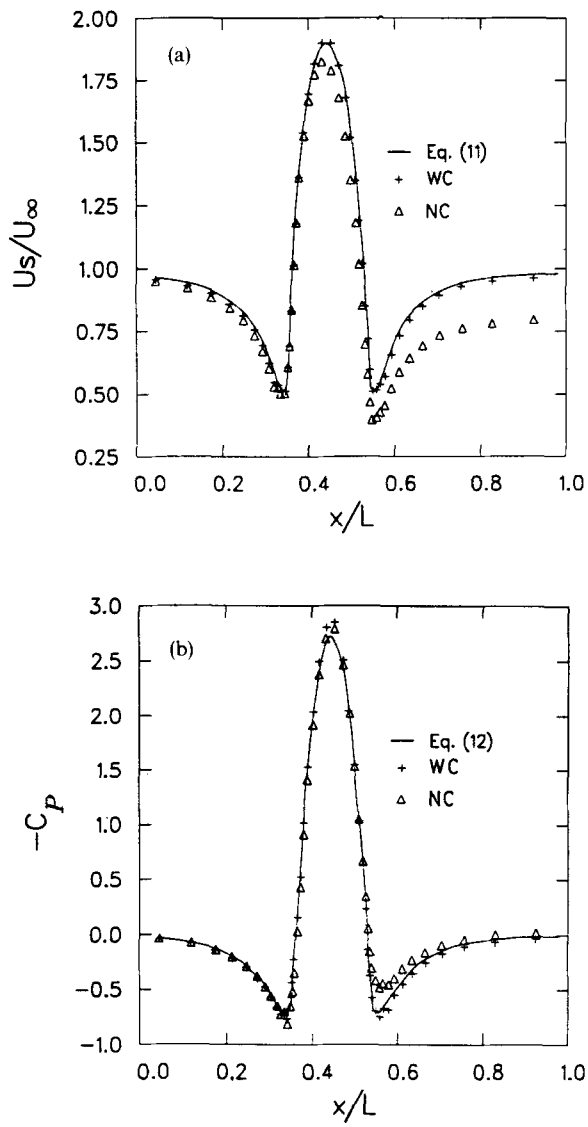

Figure 6. Comparison of numerical and analytical solutions for potential flow past a cylinder: (a) streamwise velocity distribution along plane of symmetry and cylinder surface; (b) pressure coefficient distribution along plane of symmetry and cylinder surface

The pressure error as well as the false diffusion error can be eliminated[13] if U_e is determined from interpolation using U_P and U_E (central difference approximation), from extrapolation using U_P and U_W (second-order upwind assuming $U_e > 0$), or by using parabolic interpolation (QUICK assuming $U_e > 0$). While such schemes yield good accuracy, at least on fine meshes,[14] the profile shape does not adjust to reflect the importance of the different physical processes. This leads to algebraic equations with transport properties that are different from those of the underlying differential equations. This in turn leads to solutions that often have non-physical oscillations. The method proposed in this paper yields well conditioned equations and solutions which have a lower propensity for 'wiggles'.

Calculations performed for laminar flow in a converging–diverging duct and for potential flow past a cylinder indicate that the application of the correction allows a significant reduction in the total pressure error and an improvement in the numerical solution.

APPENDIX: NOMENCLATURE

a	radius of cylinder (Figure 5)
C_p	pressure coefficient (equation (12))
e	fluid strain
h_1, h_2	grid metrics in the x_1- and x_2-direction respectively
L	distance between two adjacent nodes (Figure 1)
$\dot{M}$	mass flows through the faces of the control volumes
P	pressure
R	total pressure error (equation (10))
Re	Reynolds number
S	momentum source term (equation (2))
U	velocity component in the x_1-direction
U_s	streamwise velocity
U_∞	freestream velocity
V	velocity component in the x_2-direction
x_1, x_2	generalized co-ordinate directions
x, y	Cartesian co-ordinates

Greek letters

α	convective weight
ΔS_1, ΔS_2	arc lengths in the x_1- and x_2-direction respectively
Δy	control volume dimension in y (Figure 1)
μ	laminar viscosity
ρ	density

Subscripts

1, 2	denoting co-ordinate directions x_1 and x_2, respectively
e, w	referring to locations on the faces of the control volumes
P, E, W, EE	referring to nodal locations
∞	referring to freestream condition

Acronyms

WC	with correction
NC	no correction

REFERENCES

1. G. D. Raithby, 'A critical evaluation of upstream differencing applied to problems involving fluid flow', *Comput. Methods. Appl. Mech. Eng.*, **9**, 75–103 (1976).
2. I. P. Castro, K. A. Cliffe and M. J. Norgett, 'Numerical predictions of the laminar flow over a normal flat plate', *Int. j. numer. methods fluids*, **2**, 61–88 (1982).
3. P. F. Galpin, G. D. Raithby and J. P. Van Doormaal, 'Discussion of upstream-weighted advection approximations for curved grids', *Numer. Heat Transfer*, **9**, 241–246 (1986).

4. J. N. Lillington, 'A vector upstream differencing scheme for problems in fluid flow involving significant source terms in steady-state linear systems', *Int. j. numer. methods fluids*, **1**, 3–16 (1981).
5. P. F. Galpin, R. G. Huget and G. D. Raithby, 'Fluid flow simulations in complex geometries', *Second Int. Conf. on Simulation Methods in Nuclear Engineering*, Canadian Nuclear Society, Montreal, October 1986.
6. G. D. Raithby and K. E. Torrance, 'Upstream-weighted differencing schemes and their application to elliptic problems involving fluid flow', *Comput. Fluids*, **2**, 191–206 (1974).
7. M. R. Spiegel, *Mathematical Handbook*, Schaum's Outline Series, McGraw-Hill, New York, 1968.
8. D. B. Spalding, 'A novel finite difference formulation for differential expressions involving both first and second derivatives', *Int. j. numer. methods eng.*, **4**, 551–559 (1972).
9. V. De Henau, 'A numerical study of the turbulent flow around airfoils', *M.A.Sc. Thesis*, University of Waterloo, Waterloo, Ontario, 1987.
10. S. V. Patankar, *Numerical Heat Transfer and Fluid Flow*, Hemisphere, Washington DC, 1980.
11. G. D. Raithby, P. F. Galpin and J. P. Van Doormaal, 'Prediction of heat and fluid flow in complex geometries using general orthogonal coordinates', *Numer. Heat Transfer*, **9**, 125–142 (1986).
12. L. M. Milne-Thompson, *Theoretical Aerodynamics*, Dover Publications, New York, 1958.
13. G. D. Raithby and G. E. Schneider, 'Elliptic systems: finite difference method 2', in *Handbook of Heat Transfer*, Wiley, New York, 1988, Ch. 7.
14. J. P. Van Doormaal, A. Turan and G. D. Raithby, 'Evaluation of new techniques for the calculation of internal recirculating flows', *AIAA Paper 87-0059, 25th Aerospace Sciences Meeting*, Reno, 1987.